Journal of New Materials for Electrochemical Systems 14, 229-236 (2011)

Comparison of the Photoelectrochemical Characteristics of Dye-Sensitized Inverse-Opal Electrodes Prepared by Various Liquid-Phase Methods

Sachiko Matsushita[1,2,*], Chie Nishiyama[2], George Kato[2], Akira Nakajima[1], Toshihiro Isobe[1] and Takuya Hashimoto[2]

[1]Department of Metallurgy & Ceramics Science, Graduate School of Science & Technology, Tokyo Institute of Technology, 2-12-1, Ookayama, Meguro-ku, Tokyo 152-8552, JAPAN
[2]Division of Optical and Electronic Sciences, Nihon University, 3-25-40 Sakurajosui, Setagaya-ku, Tokyo 156-8550, JAPAN

Received: February 21, 2011, Accepted: May 11, 2011, Available online: May 27, 2011

Abstract: *The photovoltaic characteristics (short circuit current, open circuit voltage, fill factor, and photon-to-electron conversion efficiency) and electrochemical impedance measurements of normal and inverse-opal dye-sensitized electrodes were carried out in a transparent electrolyte (0.6 M triethhanolamine/0.5 M lithium perchlorate in acetonitrile) using three different methods; electrophoretic deposition, $TiCl_4$ coating, and liquid-phase deposition (LPD). X-ray diffraction (XRD) analysis revealed that each electrode was composed of anatase TiO_2. The impedance elements discussed previously were substrate resistance (R_0), interface resistance at indium tin oxide (ITO)/titanium oxide (TiO_2) (R_1), contact resistance between TiO_2 particles (R_2), interface resistance at TiO_2/dye/electrolyte and counter electrode/electrolyte (R_3), and diffusion resistance of the electrolyte (R_4). The internal resistances of inverse opal electrodes were varied with the preparation methods, especially in relation to the contact resistance between R_2 and R_3. The electrode prepared by LPD exhibited the smallest internal resistances and the highest photon-to-electron conversion efficiency among the three methods.*

Keywords: self-assembly; photonic crystal; colloidal crystal; self-assembled particle structure; photoelectrode

1. INTRODUCTION

An inverse opal [1-7], a kind of self-assembled photonic crystal, has been applied in dye-sensitized electrodes with a view to improving the light-harvesting effect [8]and photon-inhibition effect [3,9]. Packings of submicrometer-sized spheres were initially used as highly diffusive reflecting layers [10]. In 2003, an inverse opal was employed as a novel optical element to further improve the efficiency of DSSCs and was reported on by Mallouk [11]. An enhancement of up to 26% of the photogenerated current efficiency of the DSSCs was achieved compared to the standard ones by coupling a TiO_2 inverse opal layer to a conventional DSSC. In later research Mallouk reported that the bilayer architecture, rather than enhanced light harvesting within the inverse opal structures, was responsible for the bulk of the gain in photogenerated current efficiency [12]. Conversely, a theoretical investigation by Miguez et al. revealed that the effect of the presence of an inverse opal on the optical absorption of the DSSC was mainly the consequence of partial localization of light within the TiO_2 layer and there was no need to sensitize the scattering layer; efficient absorption could be attained as long as a highly reflective inverse opal was implemented [13,14]. Miguez suggested that slow photon resonant modes or photon localization partially confined within the absorbing part of a cell by the mirroring behavior of the photonic superlattice was the origin of the observed efficiency enhancement in photonic-crystal-coupled DSSCs, and a large efficiency enhancement of about 60% in a broad spectrum range (450-720 nm) should be possible. Very recently, Tao et al. theoretically predicted that the combination of the photon localization mode and the double layer scattering as mirrors lead to efficient enhancement of the absorption of DSSCs in the whole visible spectrum (400-800 nm) and a distinct increment of about 80% of photocurrent efficiency with respect to standard cells [4].

However, it is currently thought that the effect of inverse opals

*To whom correspondence should be addressed:
Email: matsushita.s.ab@m.titech.ac.jp
Phone: +81-3-5734-2525, FAX: +81-3-5734-3355

as DSSCs were still ambiguous because the above reports had not discussed the electrochemical internal resistances of the inverse opals. It should be noted that the obtained photon-to-electron conversion efficiency of inverse opals (without nanocrystalline layers) was relatively low (~3.7 % [15]). This result suggests that the mass transport of electrolyte ions, which is not a major source of loss in high performance cells, should be significant in the inverse opal electrodes. An understanding of the internal resistances of the inverse opals would accelerate the understanding of the photonic-crystal photoelectrodes. The current research is the report on the electrochemical impedance of DSSCs in a transparent electrolyte coupling to inverse opals prepared by three practical methods; electrophoretic deposition [16], $TiCl_4$ coating [17], and liquid-phase deposition (LPD) [11], as well as their photovoltaic characteristics; short-circuit current density (J_{SC}), open-circuit voltage (V_{OC}), fill factor (FF), and photon-to-electron conversion efficiency (η). Five impedance elements; substrate resistance, interface resistance at indium tin oxide (ITO)/titanium oxide (TiO_2), contact resistance between TiO_2 particles, interface resistance at TiO_2/dye/electrolyte, interface resistance at a counter electrode/electrolyte, and diffusion resistance of electrolyte, are discussed in conjunction with the results of scanning electron microscopy (SEM) and X-ray diffraction analysis (XRD).

2. EXPERIMENTAL

2.1. Preparation of artificial opals with polystyrene particles

Artificial opals were prepared by a self-assembly method using a 0.1 wt% aqueous solution of polystyrene particles (204 nm, 10 wt%, Duke Scientific Co.). Distilled water was used to adjust the suspension concentration. Twenty milliliters of the particle suspension was poured in a glass bottle (diameter 4.0 cm, height 4.1 cm). An ITO substrate (10 Ω/□, 4×3 cm^2, Geomatec Co.) was rinsed with pure water (Wako Industries, Ltd.). A silicone (Si) plate coated with platinum (Pt) was also used as an electrode substrate. The Si substrates made hydrophilic using an ozone cleaner (NL-UV253, Nippon Laser & Electronics Lab). The oxygen pressure was 0.02 Pa and the UV light exposure time was 3 min. These substrates were fixed with a clip and hung on a bamboo skewer, and then soaked in the bottle filled with the particle suspension. The dipping depth was approximately 2 cm. The glass bottles were dried at 50 °C for 5-7 days in an incubator (DRN420DA, Toyo Seisakusho Co.) while the water composed of the particle suspension was completely evaporated.

2.2. Preparation of TiO_2 inverse opals

The inverse opals with TiO_2 were prepared by three methods: electrophoretic deposition, $TiCl_4$ coating and LPD. As the references, TiO_2 electrodes without opal (normal electrode) were also prepared on bare ITO substrates by the three methods.

2.2.1. Electrophoretic deposition

The prepared artificial opals were soaked in a 10% metatitanic acid slurry (Sakai Chemical Industry Co.). Constant voltage of 1 V was applied for 30 sec by a potentiostat (HSV-100, Hokuto Denko Co.). The counter electrode was a Pt electrode. The substrates after the electrophoretic deposition were dried in air at room temperature, and sintered at 500 °C for 1 h in air with a heating rate of 0.8 °C/min (KDF-S70, Denken Co.) to calcinate the template and anneal the TiO_2.

2.2.2. $TiCl_4$ coating

Ten microliters of 2% titanium (IV) chloride ($TiCl_4$, Wako Industries, Ltd.) in methanol was added using a micropipette onto a 2×2 cm^2 artificial opal surface. The hydrolysis spontaneously occurred at room temperature within 30 min. After hydrolysis, the sample was heated to 80 °C in air. This drop-and-dry process was repeated three times to ensure the filling of all voids. Finally, the sample substrate was sintered at 500 °C for 1 h in air with a heating rate of 0.8 °C/min (KDF-S70, Denken Co.)[18].

2.2.3. Liquid-phase deposition (LPD)

The artificial opals were soaked in a 0.15 wt% titanium isopropoxide ($((CH_3)_2ChO]_4Ti$, 95.0%, Wako Industries, Ltd.) in ethanol/0.015% nitric acid (HNO_3, Wako Industries, Ltd.) solution for 5 min., and dried in air at room temperature [19]. Subsequently, the substrates were soaked in an aqueous solution of 0.1 M ammonium hexafluorotitanate ($(NH_4)_2TiF_6$, Wako Industries, Ltd.) and 0.2 M boric acid (H_3BO_3, Wako Industries, Ltd.) at 60 °C for 30 min. The pH of the solution was adjusted to approximately 3 by adding hydrochloric acid (Wako Industries, Ltd.). The substrates were rinsed with pure water and dried in air at room temperature, and sintered at 500 °C for 1 h in air with a heating rate of 0.8 °C/min (KDF-S70, Denken Co.).

2.3. SEM observation

The electrodes were observed using an SEM (S-5200, Hitachi).

2.4. XRD measurement

X-ray powder diffraction (XRD) measurements were carried out on the inverse opals using an X-ray diffractometer (50 kV, 250 mA, RINT2500 VPC, Rigaku) equipped with a graphite monochromator using the Cu Kα line (λ = 1.54 Å) at room temperature from 10 to 50° at 0.02 steps, and the results were compared with the database of the Joint Committee on Powder Diffraction Standards (JCPDS)[20].

2.5. Dye adsorption

Chlorine e6 trisodium salt (Chl, $C_{34}H_{33}N_4O_6 \cdot 3Na$, Tama Biochemical Co.) was used as the dye for the DSSCs[21]. The prepared inverse-opal electrodes were heated on a hot plate (HP-400A, Azuwan Co.) at 200 °C for 10 min. After heating, the electrodes were dipped in 3×10^{-4} M dye/30 mM chenodeoxycholic acid ($C_{24}H_{40}O_4$, Wako Industries, Ltd.) methanol solution at 15 °C for about 1 day.

2.6. Measurements of photovoltaic characteristics and electrochemical impedance

A silicon rubber (2×2×0.1 cm^3) with a hole of 3 mm radius was used as the spacer. The spacer was put on the inverse-opal electrode. An electrolyte (0.6 M triethanolamine ($N(CH_2CH_2OH)_3$, Wako Industries, Ltd.)/0.5 M lithium perchlorate ($LiClO_4$, Wako Industries, Ltd.) in acetonitrile) was poured in the hole. A Pt sheet (2×3 cm^2) was used as a counter and reference electrode. The cell was connected to a potentiostat (HSV-100, Hokuto denko) for the measurement of photovoltaic characteristics and a potentiostat/galvanostat (VersaSTAT 3, Toyo Co.) for the impedance meas-

urement at open circuit voltages. Light (AM 1.5) was illuminated on the ITO side of the cell using a solar simulator (JASCO Co.). The measured frequency was 1 Hz-10 kHz and the effective voltage was 10 mV. The obtained data was analyzed from the Nyquist diagrams using the software Z-View for Windows. Whole measurements were carried out at room temperature.

3. RESULTS AND DISCUSSION

3.1. Quality of the artificial opals

The artificial opal exhibited a light blue color when viewed with the naked eye. The sample area was 1.5×2 - 2×2 cm^2. Several artificial opals had stick-slip patterns[22]. The contact angle of the bare ITO substrate after hydrophilic treatment was 79.2±1.60°, as measured by the tangent line method. The SEM observation revealed that the number of layers in the artificial opal was over 20 (Figure 1). Several defects were observed in the artificial opals; however, it can be said that the particles in the artificial opals were well ordered as a base material for the preparation of inverse opals.

3.2. The quality of TiO_2 inverse opals

The inverse opals prepared by different methods exhibited eminent differences even with the naked eyes. The details are as follows.

3.2.1. Electrophoretic deposition

The colloidal particles in a water solution generally have negative charges; consequently, the nanoparticles were deposited on a substrate with an applied positive bias. The substrate prepared by the electrophoretic deposition was white. The void diameter in the inverse opal was approximately 226.7±5.8 nm. The thickness of the inverse opal and normal electrode was 600 nm. It seems that some parts of the TiO_2 inverse opals were exfoliated from the substrate when the artificial opals were soaked in a metatitanic acid slurry because the slurry had high viscosity. The exfoliated length was around 5 mm in the worst case and became more extensive after applying the voltage. This was thought to have been caused by the electro-decomposition of water owing to the applied voltage of over 1 V, resulting in the generation of oxygen and hydrogen gases on the ITO substrate.

Our metatitanic acid slurry was composed of crystalline titanium particles (around 14 nm). Thus, in the case of the artificial opals prepared using small polystyrene particles (such as 200 nm diameter in our experiments), titanium particles could not enter the small spaces between the polystyrene particles. Even if some titanium particles could enter the small spaces, the contact area between the titania particles would be small, resulting in the easy collapse of the inverse opals. For this reason, electrophoretic deposition may not be the best method for deposition on the artificial opals composed of small polystyrene particles.

3.2.2. $TiCl_4$ coating

The substrates prepared by $TiCl_4$ coating exhibited a white-yellow iridescent color. The void diameter in the inverse opals was 180.9±3.5 nm. The thickness of the inverse opal was over 3 μm. The TiO_2 film prepared by $TiCl_4$ coating had a honeycomb-like structure (Figure 2b). This was thought to be caused by the low viscosity of the $TiCl_4$ solution, resulting in the deep intrusion into the artificial opal. The low viscosity also became a disadvantage.

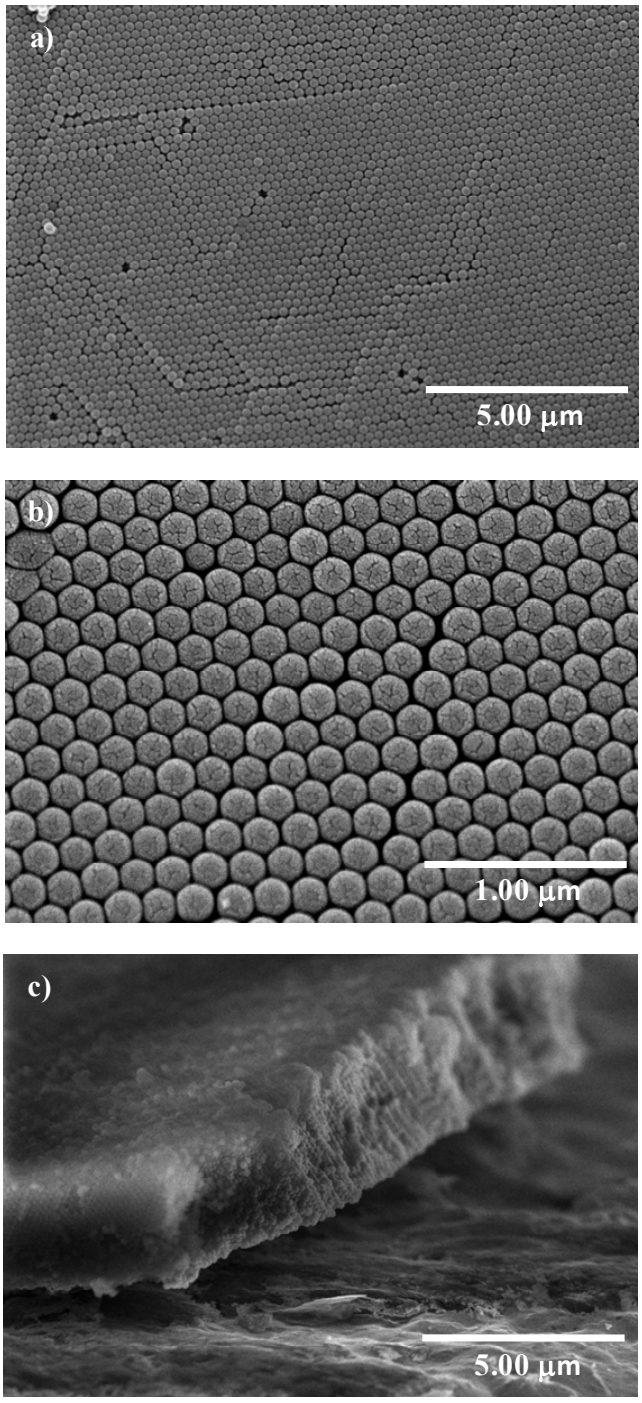

Figure 1. Scanning electron microscopy images of (a, b) the surface and (c) the cross section of self-assembled polystyrene particle structures.

The $TiCl_4$ solution was difficult to adsorb onto the polystyrene particle surface during the intrusion. Thus, the inverse opal structure had a honeycomb-like networked structure, instead of the multi-spherical air atoms.

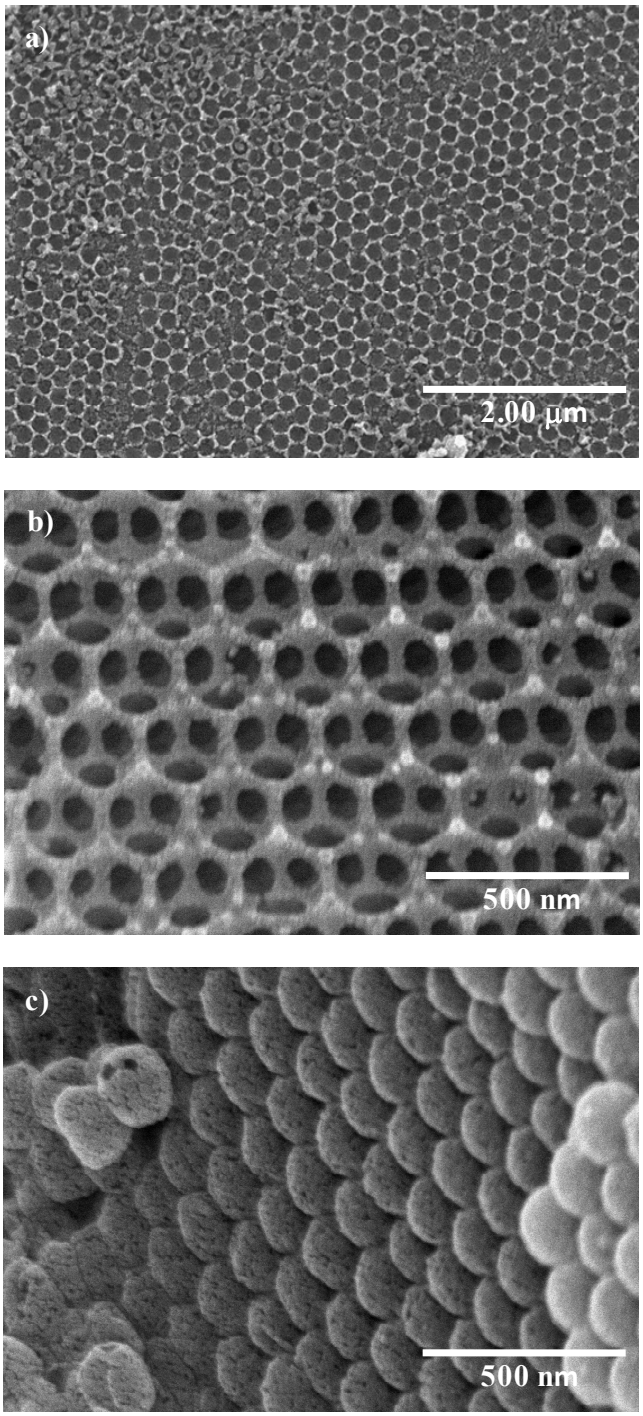

Figure 2. Scanning electron microscopy images of various inverse opals prepared by (a) electrophoretic deposition, (b) TiCl4 coating, and (c) liquid-phase deposition (LPD).

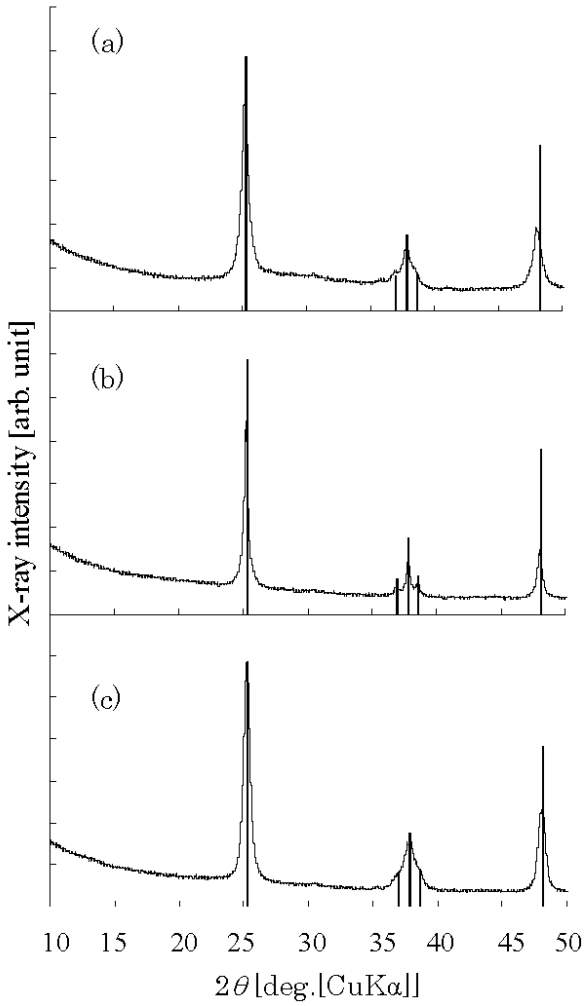

Figure 3. X-ray diffraction patterns of the inverse-opal electrodes prepared by (a) liquid phase deposition (LPD), (b) TiCl4 coating, and (c) electrophoretic deposition. The peaks of the anatase-type TiO2 are indicated by black straight lines.

3.2.3. Liquid Phase Deposition

The substrate prepared by LPD exhibited a yellow iridescent color. Any difference with the substrate prepared by $TiCl_4$ coating was not visible with the naked eye. However, SEM observations revealed that spherical air atoms were formed in the inverse opals prepared by LPD. The void diameter in the inverse opal was 196.3±5.5 nm. The thickness of the inverse opal was over 3 μm, almost same with $TiCl_4$ coating. The formation of the spherical atoms suggests that each polystyrene particle was well coated with $TiCl_4$ solution (Figure 2c). $TiCl_4$ coating and LPD include hydrolysis. The $TiCl_4$ process was carried out in air; in contrast, LPD was carried out in a controlled pH solution at 60°C. Thus, in the LPD process, we could control the electric double layer on the titania particles, resulting in the formation of the fine mold of artificial opal structure.

3.3. XRD measurements

XRD measurements were carried out to confirm the crystalline type of TiO_2 in the inverse opals (Figure 3). The electrodes prepared by these three methods were composed of only anatase-type TiO_2.

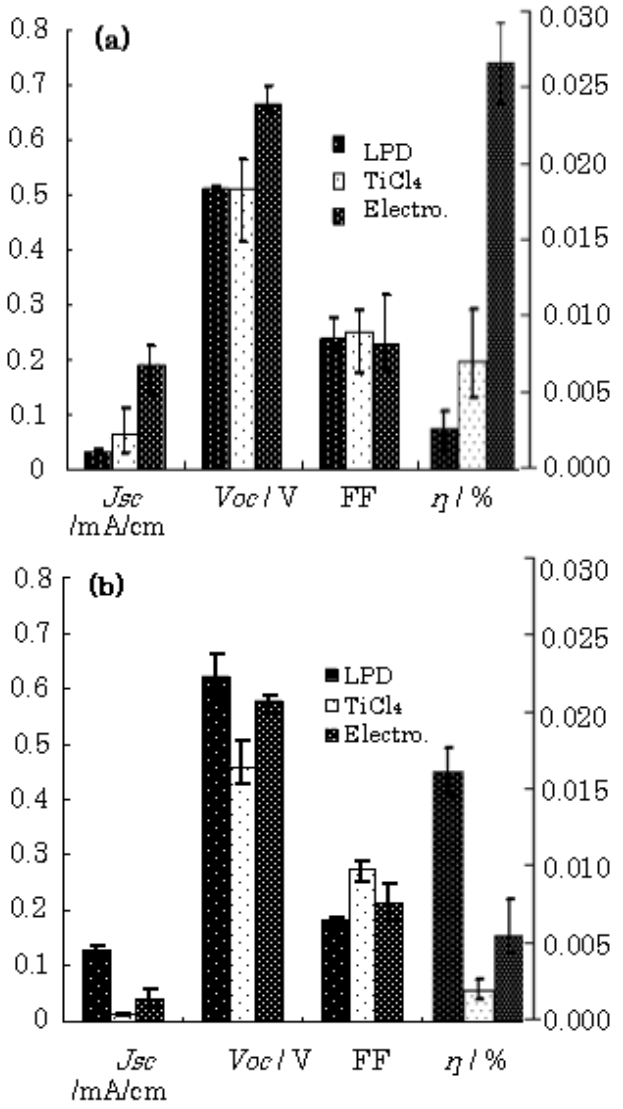

Figure 4. Photovoltaic characteristics of normal dye-sensitized electrodes (a) and dye-sensitized inverse-opal electrodes (b) prepared by LPD, TiCl4 coating, and electrophoretic deposition. The left y-axis is for Jsc, Voc, and FF, and the right y-axis is for η.

3.4. Photovoltaic characteristics and Electrochemical Impedances

The photovoltaic characteristics; short-circuit current density (J_{SC}), open-circuit voltage (V_{OC}), fill factor (FF), and photon-to-electron conversion efficiency (η) of flat electrodes and inverse-opal electrodes prepared by various methods are shown in Figure 4. It is important to discuss those photovoltaic characteristics with consideration of our electrochemical impedance results (Figure 5).

With reference to the equivalent circuit model for ac impedance spectroscopy in the analysis of DSSCs, Hoshikawa, et al. discussed five resistance elements (discussed below)[23]. Han et al. discussed four resistance elements (substrate resistance, counter-electrode resistance, TiO_2/dye/electrolyte interface, and Nernstian diffusion within the electrolyte)[24][25] in DSSCs. The relationship between the DSSC's photovoltaic characteristics and internal resistances were precisely reviewed by Koide et al. with the view of complete cell design using the conventional *pn*-junction solar cell concept[25]. Here, our equivalent circuits of the impedance spectrum followed Hoshikawa's equivalent circuit, because we would like to focus on the resistances of the TiO_2 electrode rather than total cell resistances.

In the circuit (Figure 5a), we used the resistance (R), capacitance (C) and constant phase element (CPE). The CPE is generally used as the capacitance of porous surfaces as are our electrodes (Fig. 1). Here, we would like to focus on R, rather than the capacitance factors. The Cole-Cole plots of the normal and inverse opal DSSCs are depicted in Figures 5b and 5c. Our Cole-Cole plots were not observed as arc shapes, as are frequently presented in other papers, because the resistances in the low frequency range was not measured in our experiments. The average, maximum, and minimum experimental *R* values in the normal and inverse-opal DSSCs are plotted in Figures 5d and 5e, respectively. The element at ~5 Hz, which is presented as R_0 in Figure 5, should be attributed to the ITO substrate because this resistance was less observed when a Pt-coated Si substrate was used. Thus, R_0 is not discussed in this paper. The R_1 at approximately ~7.5 kHz was reported as the impedance factors at the substrate/TiO_2 interface. The R_2 at approximately ~750 Hz was the impedance factors between TiO_2 particles. R_3 at approximately ~10 Hz was the impedance factors at the Pt/electrolyte interface and electrolyte/dye/TiO_2 interface. Diffusion resistance of the electrolyte (R_4) was also confirmed at ~0.3 Hz.

3.4.1. Normal electrodes

Let us start our discussion from J_{SC}. The J_{SC} of the electrodes prepared by LPD and $TiCl_4$ coating were relatively small (~0.05 mA/cm^2). On the other hand, the J_{SC} of the electrodes prepared by electrophoretic deposition was large (~0.2 mA/cm^2). The electrode surface prepared by electrophoretic deposition was covered by aggregated metatitanic acid particles (the original particle diameter was ~20 nm) during the preparation process. The aggregation formed a larger surface area than those prepared by other methods. This larger surface area may be one of the reasons for such a large J_{SC}.

The internal resistance of the cell is also an important factor when discussing the J_{sc}. The R_4 value was strongly dependent on the preparation method employed (Figure 5 d). The R_4 of the normal electrode prepared by LPD was more than double that of other electrodes. In our electrodes, macro pores(> 50 nm) were observed at the electrode surface prepared by $TiCl_4$ coating and electrophoretic deposition (Figure 2). Micro-(< 2 nm) and meso(2-50 nm) pores were dominant at the normal electrode surface prepared by LPD. It is considered that the smaller pore size is a contributing factor toward such a large R_4. This hypothesis was supported by the fact that the R_4 of inverse opal electrodes, which were composed of electrolyte atoms as macro pores, were approximately equal (Figure 5e). It should be mentioned that our R_4 values were larger than other reported results; this is thought to be because of our thick spacer. It can be concluded that electrophoretic deposition is the best method to employ in preparation of larger J_{sc} for flat electrodes.

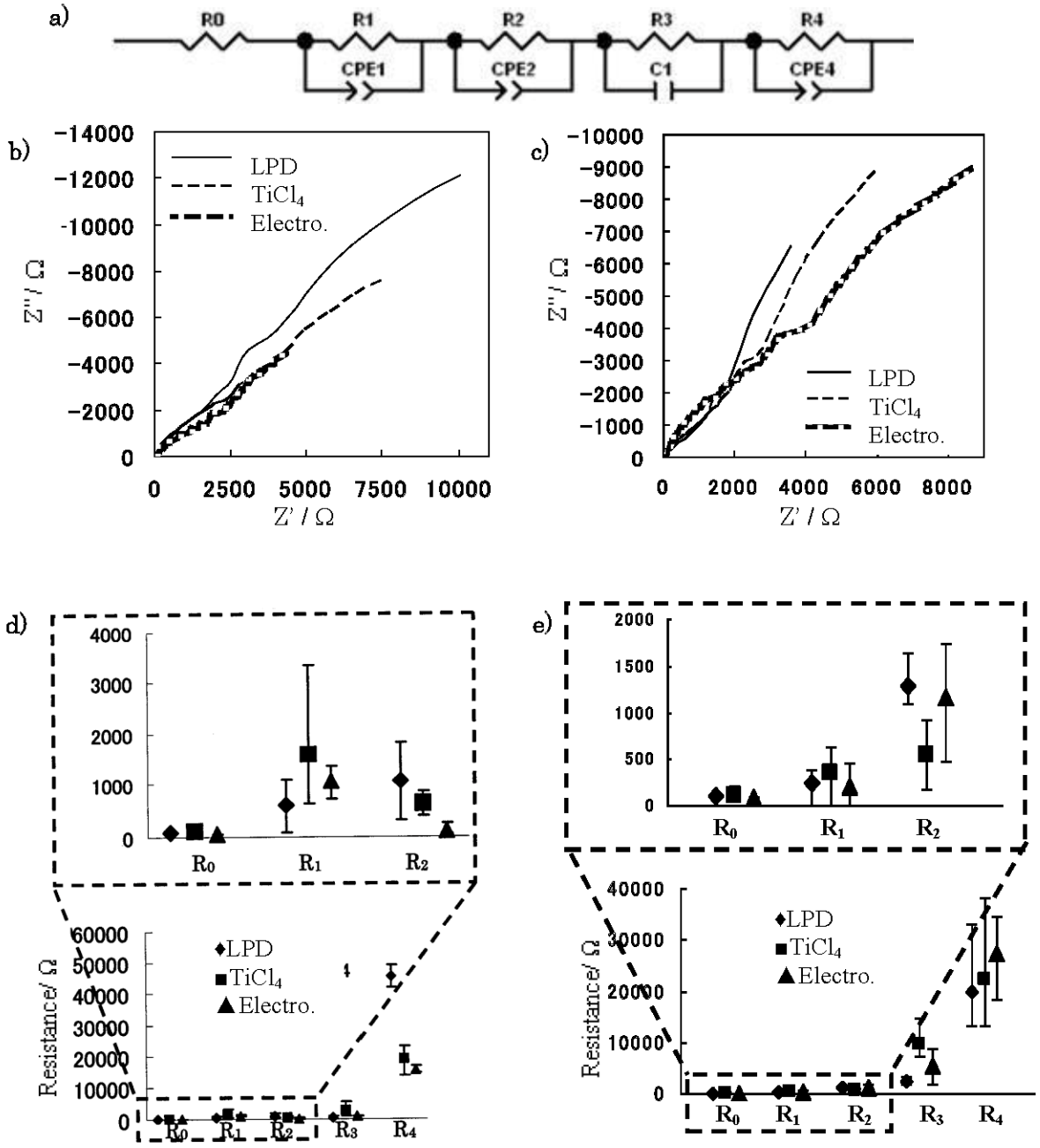

Figure 5. Equivalent circuit model of the electrochemical impedance (a), cole-cole plots of the normal electrodes (b) and of the inverse-opal electrodes (c), resistance elements in the normal electrodes (d) and in the inverse-opal electrodes (e). R0; resistance at substrate. R1; resistance at substrate/TiO2 interface, R2; resistance between TiO2 particles, R3; resistance at Pt/electrolyte interface and electrolyte/dye/TiO2 interface, R4; Diffusion resistance of the electrolyte. The electrodes were prepared by LPD, TiCl4 coating and electrophoretic deposition.

V_{oc} is essentially decided by the Fermi levels of TiO_2 (~-0.2 V vs. NHE) and the energy levels of redox ion couples in the electrolyte. Instead of redox ion couples, a transparent electrolyte, $LiClO_4$ in acetonitrile, was used so as to ignore the absorbance wavelength dependence of the electrolyte. Thus, our open circuit voltage was dependent on the transparent electrolyte ion conductivity[26]. The V_{oc} of our electrodes prepared by LPD and $TiCl_4$ coating were approximately 0.55 V, which were smaller than that of the electrode prepared by electrophoretic deposition (0.65 V) (Fig.4a). The XRD spectra suggest that all our electrodes are anatase TiO_2 and have less amorphous character (Fig. 3). The impedance results suggested that R_2 of the electrode prepared by LPD and $TiCl_4$ coating was larger than R_2 of the electrode prepared by electrophoretic deposition (Fig. 5d). The TiO_2 particles in the wall prepared by electro-

phoretic deposition are thought to have large contact area. The R_3 and R_4, (which are related to the electrolyte ion conductivity[27]) of the electrode prepared by electrophoretic deposition exhibited the smallest values. These smaller resistances may cause a larger open circuit voltage of the electrode prepared by electrophoretic deposition.

The chemical modification on the electrode surface is also discussed as a factor that affects V_{oc}. However, in our experiments, the same tendency was not observed between normal electrodes and inverse-opal electrodes from the perspective of the preparation methods. We may ignore the influences of chemical modification in our experiments. It can be concluded that electrophoretic deposition is the best in relation to obtaining larger V_{OC} for flat electrodes.

The FF values of the normal electrodes provided no clear point of difference (Fig. 4a). FF value depends on the shape of the *I-V* curve. Sometimes it became larger even with larger internal resistances. The electrode prepared by electrophoretic deposition exhibited the largest η, followed by the electrodes prepared by $TiCl_4$ coating and LPD, respectively. This result is a combination of J_{sc} and V_{oc} and suggests that electrophoretic deposition is the best preparation method among those three methods for flat electrodes in terms of the aforementioned parameters.

3.4.2. Inverse-opal electrodes

The normal and inverse-opal electrodes exhibited some differences in their electrochemical impedance characteristics similar to their photovoltaic characteristics. Here it should be mentioned that R_1, the substrate/TiO_2 interface resistance, of the inverse-opal electrodes exhibited a similar tendency to that of the flat electrodes.

Unlike the normal electrodes, the inverse-opal electrode prepared by LPD exhibited the largest J_{SC} (Fig.4b). The inverse-opal prepared by LPD was considered to be a better replica of the artificial opals and had a larger surface area than other inverse opals (as shown in Figure 2) resulting in a larger J_{SC}. On the other hand, the inverse-opal electrode prepared by $TiCl_4$ coating, comprised of tens of layers, produced a lower photocurrent than the electrode prepared by electrophoretic deposition, constructed of few layers. Generally, the J_{SC} should increases as the thickness increase because of the increase of the incident light absorption in the case of less than 10 μm thickness. The reason for the low photocurrent of the inverse opal electrodes prepared by $TiCl_4$ coating is expected from their resistances. The inverse-opal electrode prepared by $TiCl_4$ coating had the largest R_3; electroyte/dye/TiO_2 interface resistance (Fig. 5e), which has the greatest effect on the photocurrent and short circuit current. The large R_3 value may be one of the influencing factors on the low J_{sc} of the electrode prepared by $TiCl_4$ coating. It can be concluded that LPD was the best method when considering obtaining a larger J_{sc} for inverse opal electrodes.

The inverse-opal electrode prepared by $TiCl_4$ coating exhibited the lowest V_{oc} (0.5 V). As described above, our electrodes were not composed of amorphous components (Fig.3). Thus, this low V_{oc} was caused by internal resistance. In regards to the preparation methods, the difference in R_3 became more eminent among the inverse-opal electrodes compared to those of the normal electrodes (Fig. 5d and 5e). The R_3 of the inverse-opal electrode prepared by $TiCl_4$ coating was more than twice the R_3 of the normal electrode prepared by the same method, resulting in a lower V_{oc}. It can be concluded that LPD is the best method for obtaining a larger V_{oc}.

The *FF*s of normal electrodes exhibited almost equal values; however, large differences were found in those of inverse-opal electrodes. The inverse-opal electrode prepared by $TiCl_4$ coating exhibited the highest *FF*, even though it had the lowest J_{sc} and V_{oc} (Fig. 4). This may be because the *I-V* curves of other electrodes were far from rectangular in shape. Eventually, the η of the inverse-opal electrodes were of the same order of magnitude as J_{sc} and V_{oc}. It can be simply put that LPD is the best preparation method among those three methods for producing inverse opal electrodes.

An important point of discussion is the comparison between normal and inverse-opal electrodes. The inverse-opal electrode prepared by LPD exhibited an approximately four-fold higher efficiency than the normal electrode prepared by LPD. Conversely, the inverse-opal electrodes prepared by $TiCl_4$ and electrophoretic deposition exhibited lower efficiency compared with each normal electrode, around 1/3 and around 1/20, respectively. The inverse-opal electrode is normally imagined to have a larger surface area than that of the normal flat electrode; however, the bare ITO substrate surface in Figure 2a revealed that the surface area of the inverse opal electrode prepared by electrophoretic deposition was smaller than that of the normal electrode prepared by electrophoretic deposition.

The increase of R_2 and the increase/decrease of R_4 are expected in inverse opal electrodes in comparison to the normal electrodes. The R_2 values of inverse opal electrodes prepared by the LPD method and $TiCl_4$ coating were almost equal to that of the normal electrode prepared by each method, however, regarding the electrode prepared by electrophoretic deposition, the R_2 of the inverse opal electrode became ten times larger than that of the normal electrode. These results suggest that we should consider the influence of contact resistance between the TiO_2 particles in discussing the characteristics of inverse opal electrodes prepared by electrophoretic deposition. The R_4 values became nearly equal in the inverse opal electrodes, though the normal electrode prepared by the LPD method was two times larger than that of other normal electrodes. These results suggest that the difference in preparation methods could be ignored with a view to electrolyte diffusion in inverse opals, at least the atom size was larger than 204 nm.

The diffusion resistance was the largest resistance in both normal and inverse-opal electrodes (Figure 5). Generally speaking, this diffusion resistance has little effect on DSSC characterization[23]. It should be noted that the R_4 values of inverse-opal electrodes were equal to the normal electrodes prepared via $TiCl_4$ coating and electrophoretic deposition; those values were different in the case of LPD. The enhancement of photon-to-electron conversion efficiency combined with inverse-opal electrodes was widely discussed using various cell types theoretically[4] and experimentally[7,11,12,28,29]. It is sometimes suggested that the enhancement was caused by a nano/mesoscopic effect related to electrolyte diffusion. Our discussions in relation to R_4 suggest that we may ignore the nano/mesoscopic effect in the case of the $TiCl_4$ coating and electrophoretic deposition; but it is preferable to consider that the diffusion resistance of the inverse opal electrode became less than half that of LPD[8,30,31] for particles larger than 204 nm in diameter.

4. CONCLUSIONS

The current researched examined the photovoltaic characteristics (J_{sc}, V_{oc}, FF, and η) and the electrochemical impedance of normal electrodes and inverse-opal electrodes prepared by three methods; electrophoretic deposition, $TiCl_4$ coating, and liquid-phase deposition. All electrochemical analysis was carried out in a transparent electrolyte system. Each electrode was confirmed as anatase TiO_2 by XRD analysis. Five resistance elements were investigated in the electrodes: the substrate resistance (R_0), interface resistance at the ITO/TiO_2 interface (R_1), contact resistance between TiO_2 particles (R_2), interface resistance at the TiO_2/dye/electrolyte interface and resistance at the Pt electrode/electrolyte inInterface (R_3), and diffusion resistance of the electrolyte (R_4). The photovoltaic characters were discussed using the resistance elements.

The internal resistances of inverse opal electrodes were varied with the preparation methods, especially in relation to the contact resistance between TiO_2 particles (R_2) and interface resistances at the electrode (R_3). The LPD was the best preparation method among these three methods in regards to preparing inverse-opal electrodes using 200-nm polystyrene particles. The above results also suggested that the difference in resistance between normal and inverse-opal electrodes should not be ignored in the context of the LPD method. Further experiments, the measurement of incident photon-to-electron conversion efficiency for example, would reveal more useful information regarding with the inverse-opal electrode.

5. ACKNOWLEDGEMENTS

The authors thank Mr. Yohey Shibuya, Ms. Miho Kawai and Mr. Nobuhisa Hikichi for their valuable help. This work was partially supported by The Ministry of Education, Culture, Sports, Science and Technology (21750024), and Nihon University Strategic Projects for Academic Research (Nanotechnology Excellence).

REFERENCES

[1] J.E. Wijnhoven, Science, 281, 802 (1998).
[2] S.I. Matsushita, T. Miwa, D.A. Tryk, A. Fujishima, Langmuir, 14, 6441 (1998).
[3] S.I. Matsushita, N. Fukuda, M. Shimomura, Colloid Surf. A, 257, 15 (2005).
[4] C. Tao, W. Zhu, Q. An, G. Li, J. Phys. Chem. C, 114, 10641 (2010).
[5] J.I.L. Chen, E. Loso, N. Ebrahim, G.A. Ozin, J. Am. Chem. Soc., 130, 5420 (2008).
[6] K.A. Arpin, A. Mihi, H.T. Johnson, A.J. Baca, J.A. Rogers, J.A. Lewis, P.V. Braun, Adv. Mater., 22, 1084 (2010).
[7] S. Guldin, S. Hüttner, M. Kolle, M.E. Welland, P. Müller-Buschbaum, R.H. Friend, U. Steiner, and N. Tétreault, Nano Letters, 10, 2303 (2010).
[8] S.H.A. Lee, N.M. Abrams, P.G. Hoertz, G.D. Barber, L.I. Halaoui, and T.E. Mallouk, J. Phys. Chem. B, 112, 14415 (2008).
[9] S. Matsushita, S. Fujikawa, S. Onoue, T. Kunitake, M. Shimomura, Bull. Chem. Soc. Jpn., 80, 1226 (2007).
[10] S. Hore, C. Vetter, R. Kern, H. Smit, A Hinsch, Sol. Energy Mater. Sol. Cells, 90, 1176 (2006).
[11] S. Nishimura, N. Abrams, B.A. Lewis, L.I. Halaoui, T.E. Mallouk, K.D. Benkstein, J. van de Lagemaat, and A.J. Frank, J. Am. Chem. Soc., 125, 6306 (2003).
[12] L.I. Halaoui, N.M. Abrams, T.E. Mallouk, J. Phys. Chem. B, 109, 6334 (2005).
[13] A. Mihi, F. López-Alcaraz, H. Miguez, Appl. Phys. Lett., 88, 193110 (2006).
[14] A. Mihi, M.E. Calvo, J.A. Anta, H. Miguez, J. Phys. Chem. C, 112, 13 (2008).
[15] B. Eun, S. Kwak, W. Lee, N. Park, J. Kim, H. Lee, Adv. Funct. Mater., 19, 1093 (2009).
[16] Z.Z. Gu, S. Hayami, S. Kubo, Q. B. Meng, Y. Einaga, D.A. Tryk, A Fujishima, O. Sato, J. Am. Chem. Soc., 123, 175-6 (2001).
[17] H. Nakajima, T. Mori, Q. Shen, T. Toyoda, Chem. Phys. Lett., 409, 81 (2005).
[18] T. Ishihara, J. Tokue, T. Sano, Q. Shen, T. Toyoda, N. Kobayashi, Jpn. J. Appl. Phys., 44, 2780 (2005).
[19] S. Deki, Y. Aoi, O. Hiroi, A. Kajinami, Chem. Lett., 25, 433 (1996).
[20] S. Matsushita, A. Buffaz, E. Oikawa, T. Hashimoto, J. Nanosci. Nanotechnol., 9, 185 (2009).
[21] Y. Amao, J. Photochem. Photobio. A, 164, 47 (2004).
[22] S. Maegawa, K. Nakano, Wear, 268, 924 (2010).
[23] T. Hoshikawa, M. Yamada, R. Kikuchi, K. Eguchi, J. Electrochem. Soc., 152, E68 (2005).
[24] L. Han, N. Koide, Y. Chiba, T. Mitate, Appl. Phys. Lett., 84, 2433 (2004).
[25] N. Koide, A. Islam, Y. Chiba, L. Han, J. Photochem. Photobio. A, 182, 296 (2006).
[26] M. Rahman, M. Salleh, I. Talib, M. Yahaya, J. Power Sources, 133, 293 (2004).
[27] G.B. Appetecch, F. Groce, B. Scrosati, Electrochimica Acta, 40, 991 (1995).
[28] S. Nishimura, A. Shishido, N. Abrams, T.E. Mallouk, Appl. Phys. Lett., 81, 4532 (2002).
[29] A. Mihi, H. Míguez, J. Phys. Chem. B, 109, 15968 (2005).
[30] H. Chen, S. Chen, X.I.E. Quan, Environ. Sci. Technol., 44, 451 (2010).
[31] M.E. Harakeh, L. Halaoui, J. Phys. Chem. C, 114, 2806 (2010).